

## Article

# Parafoveal and Perifoveal Accommodation Response to Defocus Changes Induced by a Tunable Lens

Najnin Sharmin <sup>1,2,\*</sup> , Petros Papadogiannis <sup>3,4</sup> , Dmitry Romashchenko <sup>4,5</sup> , Linda Lundström <sup>4</sup>  and Brian Vohnsen <sup>2</sup> 

<sup>1</sup> Intel Ireland, Leixlip Campus, W23 CX68 Kildare, Ireland

<sup>2</sup> Advanced Optical Imaging Group, School of Physics, University College Dublin, D04 V1W8 Dublin, Ireland; brian.vohnsen@ucd.ie

<sup>3</sup> 2Eyes Vision SL, 28760 Madrid, Spain

<sup>4</sup> Applied Physics, KTH Royal Institute of Technology, 106 91 Stockholm, Sweden

<sup>5</sup> R&D, Johnson & Johnson Vision, 9728 NX Groningen, The Netherlands

\* Correspondence: najnin.sharmin90@gmail.com

**Abstract:** The accommodative response of the human eye is predominantly driven by foveal vision, but reacts also to off-foveal stimuli. Here, we report on monocular accommodation measurements using parafoveal and perifoveal annular stimuli centered around the fovea and extending up to 8° radial eccentricity for young emmetropic and myopic subjects. The stimuli were presented through a sequence of random defocus step changes induced by a pupil-conjugated tunable lens. A Hartmann–Shack wavefront sensor with an infrared beacon was used to measure real-time changes in ocular aberrations up to and including the fourth radial order across a 3 mm pupil at 20 Hz. Our findings show a significant reduction in accommodative response with increased radial eccentricity.

**Keywords:** accommodation; sign of defocus; aberrations; wavefront sensor; tunable lens; parafovea; perifovea; emmetropization; myopia



**Citation:** Sharmin, N.; Papadogiannis, P.; Romashchenko, D.; Lundström, L.; Vohnsen, B. Parafoveal and Perifoveal Accommodation Response to Defocus Changes Induced by a Tunable Lens. *Appl. Sci.* **2023**, *13*, 8645. <https://doi.org/10.3390/app13158645>

Academic Editor: Zhengjun Liu

Received: 26 June 2023

Revised: 13 July 2023

Accepted: 20 July 2023

Published: 27 July 2023



**Copyright:** © 2023 by the authors. Licensee MDPI, Basel, Switzerland. This article is an open access article distributed under the terms and conditions of the Creative Commons Attribution (CC BY) license (<https://creativecommons.org/licenses/by/4.0/>).

## 1. Introduction

Accommodation is the process of change in the optical power of the eye to compensate for defocus induced by different viewing distances. The amplitude of accommodation reduces with age and becomes almost zero at around 52 years of age [1], although some studies have found that this reduction can be extended up to an age of 60 or 70 years [1–3]. The accommodative response also depends on stimulus properties, such as spatial frequency content [4] and the location in the visual field [5]. In this study, we investigate the ability of the human eye to accommodate to annular stimuli presented in the parafoveal and perifoveal visual field.

Campbell concluded that foveal cones are responsible for accommodation, i.e., only when the luminance equals the cone threshold of visibility will the accommodative reflex be triggered [6]. In the case of parafoveal vision, Fincham reported that observers were unable to accommodate to a white spot of light when its width exceeded 10 arcmin and the monocular viewing angle was more than 10 arcmin away from the spot [7]. Meanwhile, Semmlow and Tinor measured parafoveal accommodative convergence response while viewing a 6 arcmin dark target at eccentricities up to 6° and found an approximately linear drop-off in response with eccentricity [8]. Similarly, Gu and Legge measured parafoveal accommodation by varying the size of a dark disc on a bright background and instructing observers to view the contour of the circle as sharp as possible at eccentricities of 1°, 7°, 15° and 30° [9]. They concluded that peripheral vision evokes accommodative responses, albeit with reduced magnitude. The same conclusion was reached by Hartwig, Charman and Radhakrishnan when measuring the peripheral accommodative response in myopes

and emmetropes [10]. When both foveal and parafoveal accommodative cues are present, a compromise in response has been reported [11,12].

The question of parafoveal accommodation is not only of fundamental interest for research but it is also directly relevant for subjects affected by central vision loss who rely partially or entirely on parafoveal vision and vision aids [13,14]. Furthermore, peripheral optics are believed to play a role in emmetropization. The image on the peripheral retina depends on the refractive errors, the state of accommodation, and environmental factors, since the surroundings are not dioptrically uniform [15,16]. One such environmental factor is an increase in indoor activities, which has been found to be a major reason for myopia prevalence in the young population [17]. So, understanding the sensitivity to defocus at different retinal eccentricities, and the corresponding effect on accommodation in various settings, may provide important insights into the mechanisms which stimulate emmetropization and myopia [18].

We recently introduced an automated method to study foveal-driven accommodation using a current-driven tunable lens (TL) in a conjugated pupil plane to introduce a random sequence of defocus step changes within the accommodative range of each observer [19]. Randomness is used to prevent subjects from learning the required response that can otherwise mask the desired signal [20]. We expand on our earlier study and report here on measurements of the accommodative response across the macula from the fovea and parafovea to the periphery for young observers to green-colored annular stimuli with visual angle radii from  $1^\circ$  to  $8^\circ$ . Other studies have used other smaller targets to examine the peripheral retina [9,12]. They have the advantage of including higher spatial frequencies but are localized to just a small area of the retina at any time. In turn, the use of annular targets benefits from including all equidistant points from the fovea simultaneously.

## 2. Materials and Methods

Figure 1 shows a schematic of the monocular vision system used to measure parafoveal accommodation. The TL (Optotune<sup>TM</sup> EL-16-40-TC-VIS-5D-C; Optotune Switzerland AG, Dietikon, Switzerland) was used to generate a sequence of negative defocus steps within the comfortable accommodative range of each subject. This range was determined manually before measurements by asking each subject to look at the target while adjusting the power of the TL via lens driver controller software (Lens driver 4/4i). The TL had a nominal response time of 5 ms and a settling time of 25 ms. The sequence of a random pattern of defocus steps was chosen to avoid memorization of the expected accommodative response. For each subject, the same random sequence was used but scaled to their accommodative range. The TL provided step defocus changes every 10 s while the subject accommodated to an annular target. The procedure was repeated for each subject with nine different radii of the annular target, viz.,  $1^\circ$ ,  $2^\circ$ ,  $3^\circ$ ,  $4^\circ$ ,  $5^\circ$ ,  $6^\circ$ ,  $7^\circ$ ,  $7.5^\circ$ , and  $8^\circ$ . No measurements were performed beyond  $8^\circ$  retinal eccentricity for any subjects.

### 2.1. Participants

Six participants with ages in the range of 23 to 34 years old took part in this study: 1 emmetrope ( $\leq -0.5$  D), 2 mild myopes ( $\leq -3$  D), and 3 moderate-to-high myopes ( $\leq -6$  D). Subjects were provided with an information leaflet and signed an informed consent form prior to measurements. Myopic subjects wore their spectacles during measurements. Table 1 shows the age, refractive error (right eye) and experimentally determined accommodative range for each subject. An autorefractor named EyeNetra<sup>TM</sup> (EyeNetra Inc., Cambridge, MA, USA) was used to determine the refractive error, which has a nominal error of 0.35 diopters.

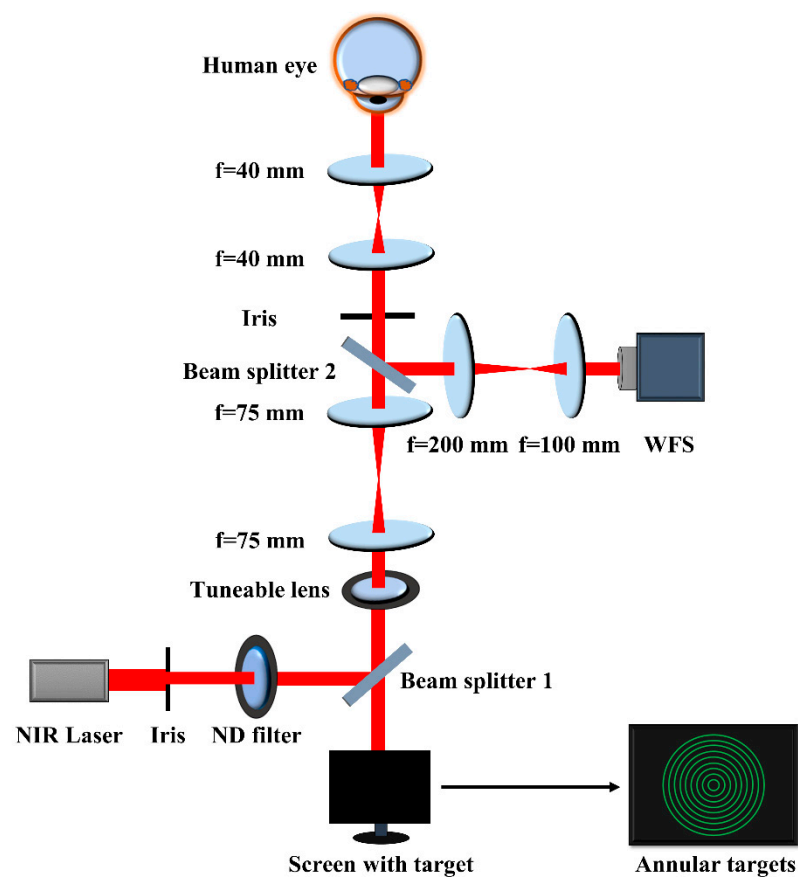


**Figure 1.** Schematic of a monocular vision system which was used to measure foveal, parafoveal and perifoveal accommodation responses to a sequence of random defocus steps. Three 4-f telescopes were used to place the iris, HS-WFS and tunable lens in conjugated pupil planes. Beam splitter 1 is a hot mirror, whereas beam splitter 2 is a 50/50 coated plate. Only a single green ring in the annular accommodation target was shown at any given time.

**Table 1.** Refractive error in diopters (D) of subjects' right eyes. The comfortable accommodative (Ac) range was determined manually with the TL for each subject. Subject #1 is an emmetrope, subjects #2 and #3 are mild myopes and subjects #4–#6 are myopes who all wore their spectacles during measurements. The visual targets were displayed on a screen placed at 1 m distance from the conjugated pupil plane (1 diopter initial bias).

Subject	Age (Years)	Sphere (D)	Cylinder (D)	Ac. Range (D)
#1	29	−0.50	0.00	3.40
#2	28	−0.75	0.00	3.53
#3	34	−0.75	0.00	2.42
#4	24	−4.75	0.00	3.35
#5	23	−5.75	0.75 (Axis 30°)	3.55
#6	25	−6.00	−2.25 (Axis 15°)	3.28

## 2.2. Procedures

Subjects viewed a green annular target on a dark background on a computer monitor with their right eye while their left eye was covered with a dark patch. The annular target, with a line width of 1.2 mm, was chosen as it simultaneously covers all points at a fixed radial distance from the fovea. For annular targets with 1°, 2°, 3°, 4°, 5°, 6°, 7°, 7.5° and 8° retinal eccentricity, the corresponding retinal illuminance was 1.51, 1.80, 1.98, 2.11, 2.21, 2.29, 2.35, 2.38 and 2.41 log Td. The monitor was placed at a viewing distance of 1 m from the conjugated pupil plane corresponding to an initial +1 diopter baseline of accommodation.

The Zernike defocus coefficient  $C_{20}$  determined with the wavefront sensor was converted from micrometers ( $\mu\text{m}$ ) to diopters (D) as follows:

$$\frac{1}{f} = -16 \times \sqrt{3} \times C_{20} / d^2, \quad (1)$$

where  $d$  is the pupil size in diameter in mm. The factor of 16 is due to the scaling of the wavefront at the pupil onto the Hartmann–Shack wavefront sensor (HS-WFS). A near-IR laser source of 850 nm wavelength (Edmund Optics™: Edmund Optics Ltd., York, UK) was focused onto the retina and served as a probe to sense real-time ocular aberrations at 20 Hz including up to the 4th radial order of the Zernike aberrations with a CMOS-based HS-WFS (Thorlabs™ WFS20-5C; Thorlabs Ltd., Ely, UK). The irradiance of the near-IR source was approximately 100  $\mu\text{W}$ . The system was computer controlled via a Labview™ interface (National Instruments Software: Labview 2016). A 3 mm iris was placed in a conjugated pupil plane to limit the effective pupil diameter to keep the measurement situation identical in all cases.

A small pupil limits the impact of higher-order aberrations and increases the depth of focus, resembling vision outdoors. In our earlier study, we found no significant difference in accommodative amplitude between pupil sizes of 2.5, 3.5 and 4.5 mm, and therefore a negligible impact of higher-order aberrations [19]. Subjects were not dilated, but the room was dark to ensure a sufficiently large natural pupil. As only changes in accommodative state were studied, a possible myopic shift caused by the dark environment, i.e., night myopia [21], was of no concern as it would provide a constant offset. A bite bar was used to limit unwanted head motion during measurements. For each of the 9 annular stimuli, the predetermined random sequence of defocus steps were induced by the TL and the subjects were instructed to look straight at the wavefront sensing beam (red dot) while keeping the circular accommodation target in focus as well as they could. To exclude disturbance by the IR beacon, separate measurements were performed without the green annular targets where the subjects were instructed to look at the red laser dot, and it was verified that the initially measured defocus of the eye did not change when the TL cycled through the defocus sequence. Thus, all subjects were able to suppress the IR beacon and concentrate on the green annular targets while using the red dot as a fixation point.

A sequence of random defocus steps was generated, and data acquisition was in each case limited to 110 s to limit fatigue. Every 5 to 10 min. subjects would rest to relax their vision and longer breaks were given if they found it difficult to accommodate. To increase comfort, data collection took place across 2 to 3 days for each subject and measurements were repeated between 2 and 3 times under certain circumstances, i.e., if the HS-WFS signal was degraded by unwanted eye motion (due to subject's head position movement) or the tiredness of subjects. In the presented data, blinks were removed numerically by using Matlab™ (MathWorks, MATLAB R2021b) processing without otherwise affecting the temporal response (shown in Figure S6), and defocus was determined as specified in Equation (1).

### 3. Experimental Results

The response to the random step sequence for subjects #1 and #2 (emmetrope and mild myope) is shown in Figure 2. For both observers, defocus changes are followed closely both during accommodation and relaxation at 1° radial eccentricity. From 2° to 6° eccentricity, accommodation and relaxation are in the expected direction but with a reduced response with increasing eccentricity, which agrees with earlier studies [10,12,22,23]. At and beyond 7° eccentricity, the accommodative response becomes negligible. The other mild myopic participant, subject #3, showed the same tendency (see Figure S1 in the supplementary document). An extra step (7.5°) between 7° and 8° radial eccentricity was taken to monitor the response closely at the point where accommodation is absent.

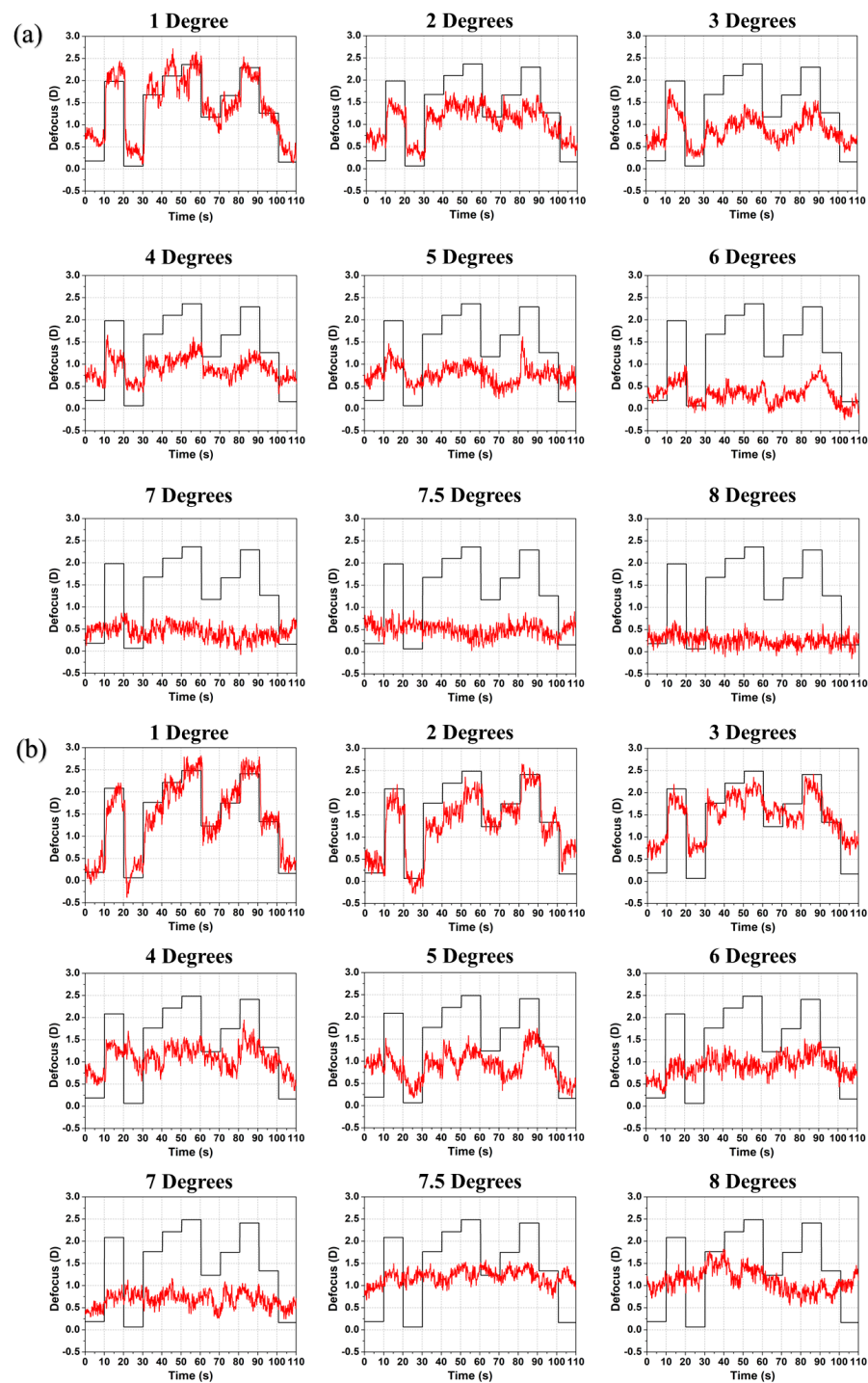


**Figure 2.** Induced defocus sequence by the TL (black line) and accommodation response (red line) as a function of time for subjects (a) #1 and (b) #2 with increasing radial eccentricity from  $1^\circ$  to  $8^\circ$ . The induced defocus is shown with opposite signs to ease comparison.

Figure 3 shows the mean accommodative response for all subjects determined for the interval of 11–19 s (induced defocus ranged from  $-1.16$  D to  $-2.10$  D depending on the individual) as a function of stimulus eccentricity for all six subjects. The accommodative response decreases with higher eccentricities, although some variations are noticeable, e.g., for subjects #2 and #3, at  $3^\circ$  eccentricity, defocus went up compared to  $2^\circ$ , and in the case of myopic subject #6, more variations were noticed at  $4^\circ$ ,  $6^\circ$  and  $7.5^\circ$ , which can be caused by overshooting or accommodation. The accommodative range and initial position differ between subjects as expected based on Table 1.



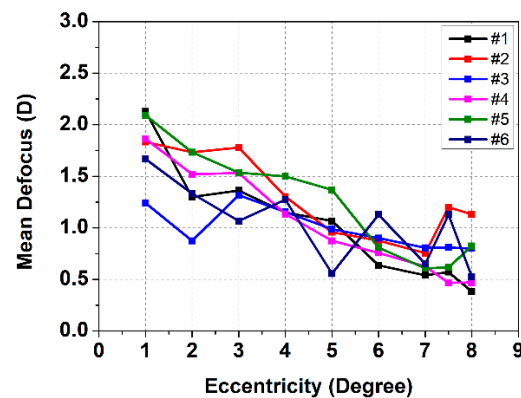


**Figure 3.** Mean accommodative response as a function of eccentricity for all subjects at the time interval of 11–19 s where the defocus induced by the TL was (#1)  $-1.98$ , (#2)  $-2.08$ , (#3)  $-1.16$ , (#4)  $-1.93$ , (#5)  $-2.10$ , and (#6)  $-1.87$  diopters.

To estimate the difference between accommodative response and induced defocus, further analysis was performed. Table 2 shows these results at the time interval of 0–110 s and radial eccentricities in the range of  $1^{\circ}$ – $8^{\circ}$  together with the average for all subjects. A low value means that the response followed the induced defocus well. Except for subject #3, all subjects showed a gradual decrease in accommodative response with eccentricity. Subject #3 is the oldest of the subjects, and therefore the range and drop-off with eccentricity is smaller. On average, the accommodative response flattens out for radial eccentricities of  $7^{\circ}$  and beyond.

**Table 2.** The average root-mean-square (RMS) deviation between induced defocus and accommodative response for all subjects for stimuli at eccentricities from  $1^{\circ}$  to  $8^{\circ}$ . The time interval was 0 to 110 s.

Subject	$1^{\circ}$	$2^{\circ}$	$3^{\circ}$	$4^{\circ}$	$5^{\circ}$	$6^{\circ}$	$7^{\circ}$	$7.5^{\circ}$	$8^{\circ}$
#1	0.388	0.628	0.802	0.805	0.956	1.259	1.247	1.222	0.925
#2	0.378	0.482	0.504	0.816	0.883	0.936	1.116	0.855	0.935
#3	0.415	0.435	0.676	0.444	0.418	0.425	0.497	0.469	0.499
#4	0.510	0.476	0.481	0.797	0.845	0.967	1.039	1.224	1.199
#5	0.476	0.499	0.719	0.671	0.842	1.112	1.294	1.258	1.185
#6	0.401	0.544	0.634	0.564	0.997	0.760	0.954	0.752	1.059
Average	0.428	0.510	0.636	0.683	0.823	0.910	1.024	0.963	0.967

To determine whether other Zernike terms were affected, selected coefficients are shown in Figure S2 for subject #1. As expected with a small 3 mm pupil, the defocus term dominates the response, although careful comparison does reveal that astigmatism  $Z_3$  changed with the same sign as  $Z_4$ , whereas astigmatism  $Z_5$  and spherical aberration  $Z_{12}$  changed with the opposite sign. This tendency was also noticed with foveal accommodation for pupil sizes up to 4.5 mm [19]. In some cases, coma  $Z_7$  and  $Z_8$  (not shown for simplicity) changed too, but only slightly (less than 0.2%), with the same sign as  $Z_4$ . In all cases, defocus alone accounts for more than 99% of the total response with a small pupil.

Figure 4 shows the accommodative response for myopic subjects #4 and #6. As emmetropes and mild myopes, myopic subjects were also able to track changes to the TL in the correct direction at up to  $6^{\circ}$  perifoveal vision, albeit with reduced response. At  $7^{\circ}$  and beyond, no response was observed (same for myopic subject #5; shown in Figure S3). The refraction by the spectacles impacts the field of view. However, for most subjects, this is a modest effect. With a vertex distance of 14 mm and for the most myopic subject (#6), wearing  $-6$  D correction equals an 8% reduction in field size (or  $7.3^{\circ}$  for the  $8^{\circ}$  target). If fully corrected with contact lenses, this will not be perceived as a reduction by the subject. Relatedly, the accommodative demand is modified by approximately 5% at  $\pm 2$  D

by accommodation [24]. All subject groups showed a similar accommodative response with smaller amplitude at increasing eccentricity and a reduced range with increased age. Some accommodative overshooting (lead of accommodation) was noted, although this occurred mostly for the untrained subjects and may thus be a result of uncertainty and increased errors.

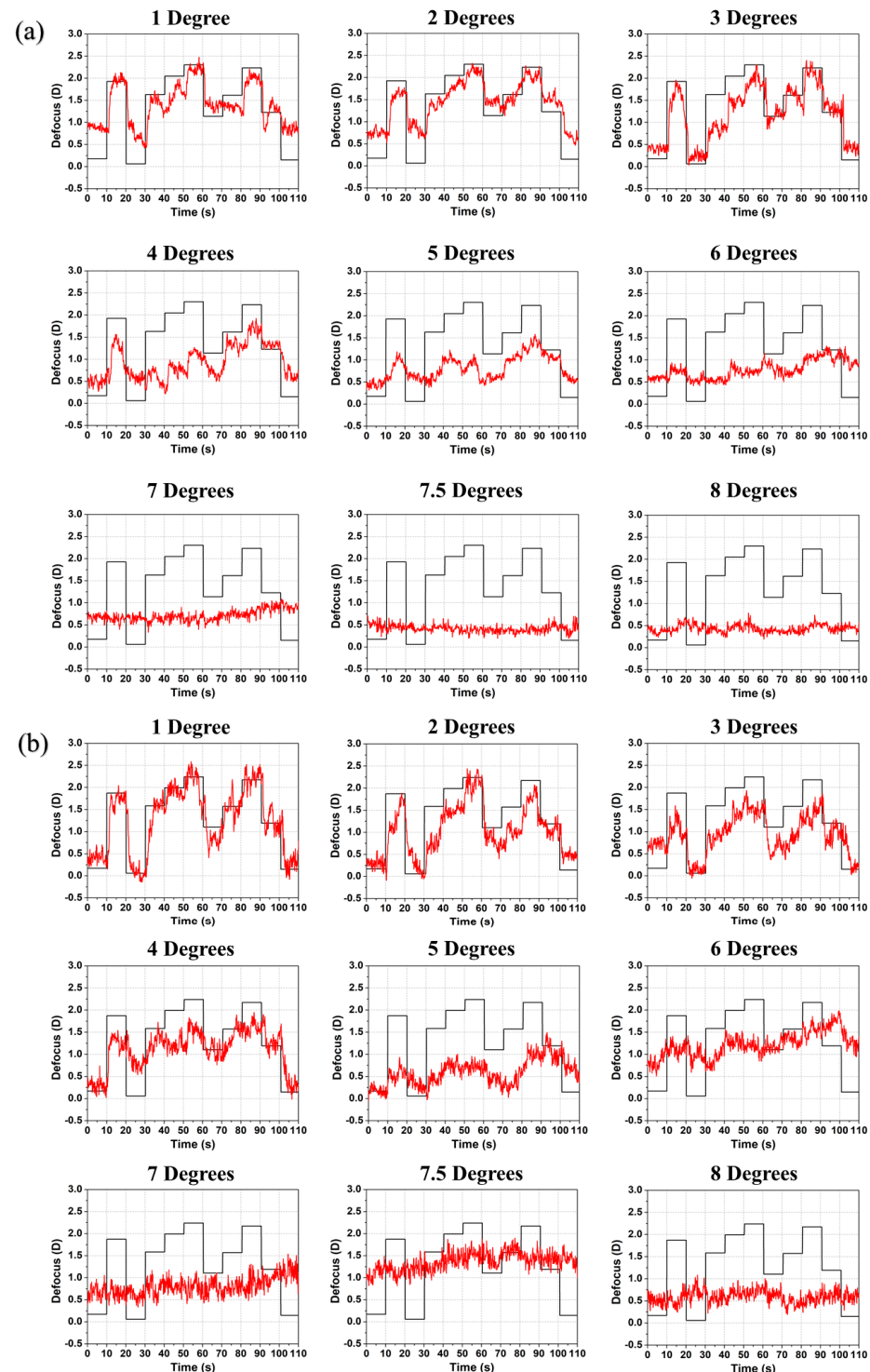


**Figure 4.** Defocus sequence induced by the TL (black line) and accommodation response (red line) as a function of time for subjects (a) #4 and (b) #6 with increasing radial eccentricity from  $1^{\circ}$  to  $8^{\circ}$ . The induced defocus is shown with opposite sign to ease comparison.

All subjects showed a similar tendency in the case of reaction and response time determined following the same procedure as in Ref. [19]. Figure 5 shows the temporal response of accommodation and relaxation for subject #1 at  $1^\circ$  and  $5^\circ$  eccentricity. The reaction time (i.e., latency or delay in the onset of accommodation) differs little between (a) lower and (b) higher eccentricities, while the response time (i.e., time required to complete accommodation before stabilizing at a new accommodative level) almost doubles at  $5^\circ$  eccentricity when compared to  $1^\circ$ , as shown in Figure 5 (and with a reduced accommodation amplitude). For foveal stimuli, the reaction time was in the range of 300–700 ms and the response time was 200–800 ms, where far-to-near accommodation response was faster than near-to-far relaxation [19,25,26]. For higher eccentricities ( $5^\circ$  and beyond), the reaction time increased slightly (400–800 ms), though some variations may occur, e.g., the relaxation reaction time is approximately 320 ms in Figure 5b, but the response time increased substantially (900 ms–2 s) for most of the cases. The response also varied with the magnitude of the induced defocus steps, but the oscillatory behavior was in good correspondence with earlier findings [27].

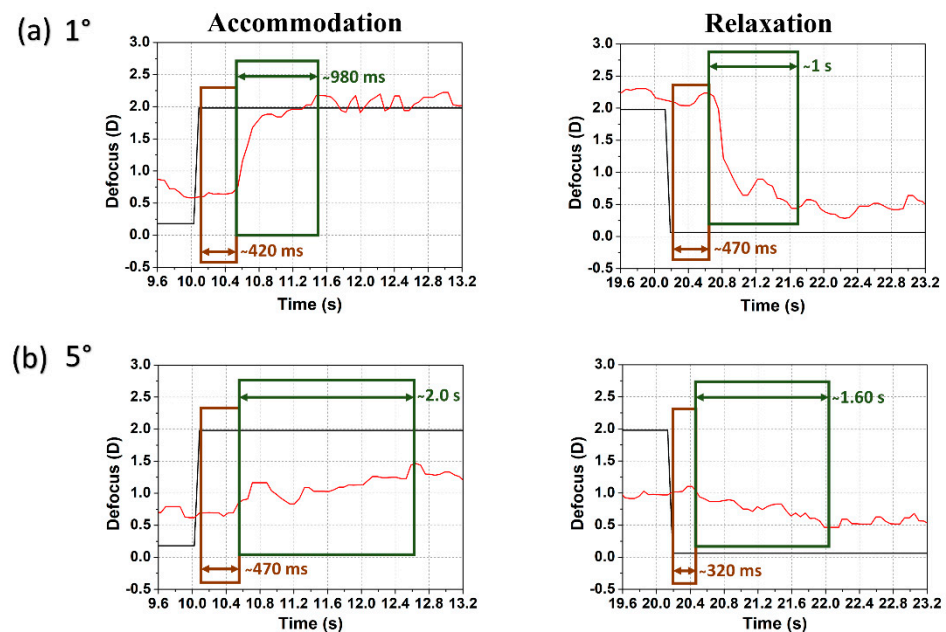


**Figure 5.** Examples of temporal dynamics with two stimulus radii (a)  $1^\circ$  and (b)  $5^\circ$ : defocus (TL: black line) and accommodation (eye: red line) following an accommodative step change (left) and relaxation (right) for subject #1. Determined reaction time (brown rectangle) and response time (green rectangle) are indicated.

Figure 6 shows examples of (a) reaction and (b) response times for subject #1 for  $1^\circ$  to  $6^\circ$  retinal eccentricity arranged from lower to higher dioptric stimulus value. Figure 6a shows an increase in reaction time at  $6^\circ$  retinal eccentricity, but there is also some variation between reaction times at other eccentricities and for different defocus stimuli. Figure 6b shows that the response time was almost 70% higher for  $5^\circ$  and  $6^\circ$  retinal eccentricity when compared to lower eccentricities. The longer times relate to the more challenging accommodation at increased eccentricity. Yet, as for the foveal study [19], there is no clear relationship between reaction and response times for different defocus stimuli. Similar observations were made for the other subjects studied (for simplicity not shown). Moreover, fatigue as well as untrained subjects would typically have increased reaction and response times. Also, increased stimulus eccentricity increases the accommodative uncertainty and required time.



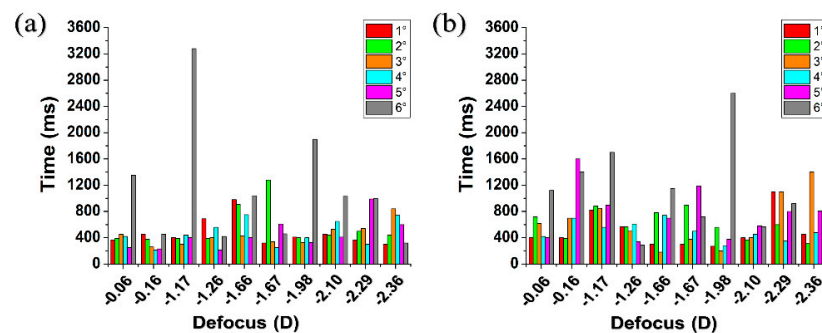


**Figure 6.** Parafoveal and perifoveal (a) reaction and (b) response times for different defocus step changes in the TL (arranged from lower to higher steps) for subject #1.

#### 4. Discussion

For all six subjects, a reduction in the parafoveal accommodation response at large eccentricity was noted, which agrees with earlier studies [8]. At 7° and beyond, there was no longer a clear correspondence between defocus stimuli and the ocular response. This is smaller than in some studies [9], plausibly due to the reduction in the number of accommodative cues when using a TL. All subjects showed similar peripheral accommodative tendencies, and therefore no more subjects were recruited in this study. A related study [12] found that at 7° retinal eccentricity (14° diameter), an accommodative response was present when subjects looked onto a black-and-white textured target made with a circle containing a Maltese cross target at the center while experiencing sinusoidal induced defocus ( $\pm 1.5$  D) caused by a TL at frequencies of 0.1, 0.2, 0.5 and 1 Hz. The presence of the central Maltese cross target can possibly be the reason why an accommodative response was still present. This differs from the methodology employed in the present study, where concentric annular targets were displayed at increasing retinal eccentricities. Accommodation is impacted by spatial frequencies, and not necessarily at the highest spatial frequencies, as shown in a study with digital blur of natural images [28]. The spatial frequency content of the annular target on a dark background is narrow when compared to that of an extended Maltese cross.

In our study, the TL induced random defocus instead of a well-known periodic defocus change, thereby reducing possible accommodative cues. Small fluctuations were noticed throughout accommodation, and it is plausible that these may provide a cue to the accommodative response [29]. Blur adaptation can improve visual acuity by approximately 0.2 logMAR within approximately an hour [30,31], and a related acuity reduction occurs after removing a prescribed correction [32]. This adaptation may partially be of optical origin, as photoreceptors dynamically adapt to the direction of incident light [22,23,33]. When it comes to the contrast of the stimuli, previous studies found that it does not have any influence on the accommodative response while reading on an electronic micro-display [34] or for near vision [35], and it has no significant impact on the accommodative lag [36]. Yet, other studies show that pupil size and higher-order aberrations may have some influence in the accommodation stimulus response [37], while illumination intensity impacts the amplitude of accommodation [38].

Another key parameter is the retinal ganglion cell density that also drops off with increasing eccentricity [39]. The parafoveal results are similar between emmetropic and myopic subjects. Thus, refractive error may matter less [40] than monocular vergence, which possibly limits the outer-segment leakage of light [41,42].

#### 5. Conclusions

In this study, we reported on an automated monocular system to measure accommodation to annular stimuli projected on the parafovea and the perifovea in response to random step defocus changes induced by a current-driven tunable lens. The accommodative response time increased gradually with increasing eccentricity, while the amplitude

decreased gradually and became negligible at  $7^\circ$  radial distance and beyond. For a 3 mm limited-eye pupil, defocus is the dominating Zernike coefficient, with no significant contribution from higher-order aberrations. Our experimental results clearly show that the amplitude of accommodation reduces with increased eccentricity, which can possibly be linked to the reduction in cone density and thus to a contrast reduction caused by the leakage of light from the outer segments [42]. Moreover, no evidence of a different accommodative response was found between subjects of different refractive errors in this study, which agrees well with previous findings [10,43]. We are conducting further research to understand the mechanisms that trigger the correct direction of accommodation and thus the detection of the sign of defocus in the young adult eye both in foveal and parafoveal vision, as this ultimately may relate to myopia and the emmetropization process [44,45].

**Supplementary Materials:** The following supporting information can be downloaded at: <https://www.mdpi.com/article/10.3390/app13158645/s1>, Figure S1: Induced defocus sequence by the TL (black line) and accommodation response (red line) as a function of time for subject #3 for increasing radial eccentricity from  $1^\circ$  to  $8^\circ$ . The induced defocus is shown with opposite sign to ease comparison; Figure S2: Individual Zernike coefficients in response to induced TL defocus changes for subject #1 for defocus  $Z_4$  (red line), astigmatism  $Z_3$  and  $Z_5$  (brown and blue lines), and spherical aberration  $Z_{12}$  (orange line); Figure S3: Induced defocus sequence by the TL (black line) and accommodation response (red line) as a function of time for subject #5 for increasing radial eccentricity from  $1^\circ$  to  $8^\circ$ . The induced defocus is shown with opposite sign to ease comparison; Figure S4: Schematic of setup to test Zernike coefficient changes in response to defocus changes of the TL monitored in a plane that is conjugate to the HS-WFS. An expanded collimated HeNe (633 nm) laser beam was used for the illumination. The iris was set to a beam diameter of 4.5 mm corresponding to the largest eye pupil used in this study; Figure S5: Changes of Zernike coefficients as a result of a random sequence of defocus changes generated with the TL as measured with the HS-WFS including up to 4th radial Zernike order. In (a) astigmatism ( $Z_3$ ,  $Z_5$ ), defocus ( $Z_4$ ), spherical ( $Z_{12}$ ), and coma ( $Z_7$ ,  $Z_8$ ) are all included on a common scale. In (b) defocus has been removed, and the vertical scale adjusted to reveal minute changes in the remaining Zernike coefficients when defocus changes; Figure S6: Analysis of blink removal with a Matlab<sup>TM</sup> code using (a) raw defocus data from the HS-WFS to obtain the (b) blink-filtered results. In (c) the difference between raw data and blink-corrected data shows no significant impact outside of the blink-induced spikes. Note that the sign of TL response has not been swapped here as it is in the main manuscript.

**Author Contributions:** Conceptualization, B.V., N.S. and L.L.; methodology, B.V. and N.S.; software, N.S. and B.V.; validation, B.V., N.S., L.L., P.P. and D.R.; formal analysis, N.S. and B.V.; investigation, N.S. and B.V.; resources, B.V. and N.S.; data curation, N.S. and B.V.; writing—original draft preparation, N.S.; writing—review and editing, N.S., B.V., L.L., P.P. and D.R.; visualization, B.V. and N.S.; supervision, B.V. and L.L.; project administration, B.V. and N.S.; funding acquisition, B.V. All authors have read and agreed to the published version of the manuscript.

**Funding:** This research was funded by European Union's H2020 ITN network "MyFUN" under Marie Skłodowska-Curie grant agreement no. 675137.

**Institutional Review Board Statement:** The study was conducted in accordance with the Declaration of Helsinki and approved by the Ethics Committee of University College Dublin Human Research Ethics Committee—Sciences (protocol code LS-16-75-Vohnsen and date of approval 12 December 2016).

**Informed Consent Statement:** Informed consent was obtained from all subjects involved in the study. Written informed consent was obtained from the patient(s) to publish this paper.

**Data Availability Statement:** The data presented in this study are available on request from the corresponding author.

**Acknowledgments:** The authors are grateful to all subjects who kindly participated in this study, and to Peter Unsbo for his discussions on the study protocol.

**Conflicts of Interest:** The authors declare no conflict of interest. The funders had no role in the design of the study; in the collection, analyses, or interpretation of data; in the writing of the manuscript; or in the decision to publish the results.

## References

1. Hamasaki, D.; Ong, J.; Marg, E. The amplitude of accommodation in presbyopia. *Am. J. Optom. Arch. Am. Acad. Optom.* **1956**, *33*, 3–14. [\[CrossRef\]](#)
2. Mordi, J.A.; Ciuffreda, K.J. Static aspects of accommodation: Age and presbyopia. *Vis. Res.* **1998**, *38*, 1643–1653. [\[CrossRef\]](#)
3. Jackson, E. Amplitude of accommodation at different periods of life. *Calif. State J. Med.* **1907**, *5*, 163–166.
4. Taylor, J.; Charman, W.N.; O'Donnell, C.; Radhakrishnan, H. Effect of target spatial frequency on accommodative response in myopes and emmetropes. *J. Vis.* **2009**, *9*, 16. [\[CrossRef\]](#)
5. Liu, T.; Sreenivasan, V.; Thibos, L.N. Uniformity of accommodation across the visual field. *J. Vis.* **2016**, *16*, 6. [\[CrossRef\]](#)
6. Campbell, F.W. The minimum quantity of light required to elicit the accommodation reflex in man. *J. Physiol.* **1954**, *123*, 357–366. [\[CrossRef\]](#)
7. Fincham, E.F. The accommodation reflex and its stimulus. *Br. J. Ophthalmol.* **1951**, *35*, 381–393. [\[CrossRef\]](#)
8. Semmlow, J.L.; Tinor, T. Accommodative convergence response to off-foveal retinal images. *J. Opt. Soc. Am.* **1978**, *68*, 1497–1501. [\[CrossRef\]](#)
9. Gu, Y.; Legge, G.E. Accommodation to stimuli in peripheral vision. *J. Opt. Soc. Am. A* **1987**, *4*, 1681–1687. [\[CrossRef\]](#)
10. Hartwig, A.; Charman, W.N.; Radhakrishnan, H. Accommodative response to peripheral stimuli in myopes and emmetropes. *Ophthalmic Physiol. Opt.* **2011**, *31*, 91–99. [\[CrossRef\]](#)
11. Hennessy, R.T.; Leibowitz, H.W. The effect of a peripheral stimulus on accommodation. *Percept. Psychophys.* **1971**, *10*, 129–132. [\[CrossRef\]](#)
12. Labhishetty, V.; Cholewiak, S.A.; Banks, M.S. Contributions of foveal and non-foveal retina to the human eye's focusing response. *J. Vis.* **2019**, *19*, 18. [\[CrossRef\]](#)
13. Timberlake, G.T.; Mainster, M.A.; Peli, E.; Augliere, R.A.; Essock, E.A.; Arend, L.E. Reading with a macular scotoma. I. Retinal location of scotoma and fixation area. *Investig. Ophthalmol. Vis. Sci.* **1986**, *27*, 1137–1147.
14. Chung, S.T.L. Enhancing visual performance for people with central vision loss. *Optom. Vis. Sci.* **2010**, *87*, 276–284. [\[CrossRef\]](#)
15. García, M.G.; Ohlendorf, A.; Schaeffel, F.; Wahl, S. Dioptric defocus maps across the visual field for different indoor environments. *Biomed. Opt. Express* **2017**, *9*, 347–359. [\[CrossRef\]](#)
16. Sprague, W.W.; Cooper, E.A.; Reissier, S.; Yellapragada, B.; Banks, M.S. The natural statistics of blur. *J. Vis.* **2016**, *16*, 23. [\[CrossRef\]](#)
17. Öner, V.; Bulut, A.; Oruç, Y.; Özgür, G. Influence of indoor and outdoor activities on progression of myopia during puberty. *Int. Ophthalmol.* **2016**, *36*, 121–125. [\[CrossRef\]](#)
18. Wallman, J.; Winawer, J. Homeostasis of eye growth and the question of myopia. *Neuron* **2004**, *43*, 447–468. [\[CrossRef\]](#)
19. Sharmin, N.; Vohnsen, B. Monocular accommodation response to random defocus changes induced by a tuneable lens. *Vis. Res.* **2019**, *165*, 45–53. [\[CrossRef\]](#)
20. Cornsweet, T.N.; Crane, H.D. Training the visual accommodation system. *Vis. Res.* **1973**, *13*, 713–715. [\[CrossRef\]](#)
21. Lopez-Gil, N.; Peixoto-de-Matos, S.C.; Thibos, L.N.; González-Méijome, J.M. Shedding light on night myopia. *J. Vis.* **2012**, *12*, 4. [\[CrossRef\]](#)
22. Eckmiller, M.S. Defective cone photoreceptor cytoskeleton, alignment, feedback, and energetics can lead to energy depletion in macular degeneration. *Prog. Retin. Eye Res.* **2004**, *23*, 495–522. [\[CrossRef\]](#)
23. Vohnsen, B. Directional sensitivity of the retina: A layered scattering model of outer-segment photoreceptor pigments. *Biomed. Opt. Express* **2014**, *5*, 1569–1587. [\[CrossRef\]](#)
24. Atchison, D.A. *Optics of the Human Eye*, 2nd ed.; CRC Press: Boca Raton, FL, USA, 2023; p. 161.
25. Charman, W.N. The eye in focus: Accommodation and presbyopia. *Clin. Exp. Optom.* **2008**, *91*, 207–225. [\[CrossRef\]](#)
26. Tucker, J.; Charman, W.N. Reaction and response times for accommodation. *Am. J. Optom. Physiol. Opt.* **1979**, *56*, 490–503. [\[CrossRef\]](#)
27. Campbell, F.W.; Westheimer, G.; Robson, J.G. Significance of fluctuations of accommodation. *J. Opt. Soc. Am.* **1958**, *48*, 669. [\[CrossRef\]](#)
28. Diez, P.S.; Ohlendorf, A.; Schaeffel, F.; Wahl, S. Effect of spatial filtering on accommodation. *Vis. Res.* **2019**, *164*, 62–68. [\[CrossRef\]](#)
29. Charman, W.N.; Heron, G. Microfluctuations in accommodation: An update on their characteristics and possible role. *Ophthalmic Physiol. Opt.* **2015**, *35*, 476–499. [\[CrossRef\]](#)
30. Williams, M.M.; Tresilian, J.R.; Strang, N.C.; Kochhar, P.; Wann, J.P. Improving vision: Neural compensation for optical defocus. *Proc. Biol. Sci.* **1998**, *265*, 71–77. [\[CrossRef\]](#)
31. Cufflin, M.P.; Mallen, E.A.H. Blur adaptation: Clinical and refractive considerations. *Clin. Exp. Optom.* **2020**, *103*, 104–111. [\[CrossRef\]](#)
32. Pesudovs, K.; Brennan, N. Decreased uncorrected vision after a period of distance fixation with spectacle wear. *Optom. Vis. Sci.* **1993**, *70*, 528–531. [\[CrossRef\]](#)
33. Carmichael Martins, A.; Vohnsen, B. Directional light-capture efficiency of the foveal and parafoveal photoreceptors at different luminance levels: An experimental and analytical study. *Biomed. Opt. Express* **2019**, *10*, 3760–3772. [\[CrossRef\]](#)
34. Bernal-Molina, P.; Esteve-Taboada, J.J.; Ferrer-Blasco, T.; Montés-Micó, R. Influence of contrast polarity on the accommodative response. *J. Optom.* **2019**, *12*, 38–43. [\[CrossRef\]](#)
35. Ward, P.A. The effect of stimulus contrast on the accommodation response. *Ophthalm. Physiol. Opt.* **1987**, *7*, 9–15. [\[CrossRef\]](#)
36. Bakaraju, R.C.; Yeotikar, N.S.; Rao, V.S. Accommodative lag versus different stimuli. *J. Mod. Opt.* **2007**, *54*, 1299–1305. [\[CrossRef\]](#)

37. Buehren, T.; Collins, M.J. Accommodation stimulus-response function and retinal image quality. *Vis. Res.* **2006**, *46*, 1633–1645. [[CrossRef](#)]
38. Kim, D.Y.; Kim, S.Y.; Hyun, H.G.; Moon, B.Y. Effects of variation of illumination on visual function factors. *J. Korean Ophthalmic Opt. Soc.* **2015**, *20*, 195–200. [[CrossRef](#)]
39. Watson, A.B. A formula for human retinal ganglion cell receptive field density as a function of visual field location. *J. Vis.* **2014**, *14*, 15. [[CrossRef](#)]
40. Lundström, L.; Mira-Agudelo, A.; Artal, P. Peripheral optical errors and their change with accommodation differ between emmetropic and myopic eyes. *J. Vis.* **2009**, *9*, 17. [[CrossRef](#)]
41. Vohnsen, B.; Carmichael, A.; Sharmin, N.; Qaysi, S.; Valente, D. Volumetric integration model of the Stiles-Crawford effect of the first kind and its experimental verification. *J. Vis.* **2017**, *17*, 18. [[CrossRef](#)]
42. Vohnsen, B. Geometrical scaling of the developing eye and photoreceptors and a possible relation to emmetropization and myopia. *Vis. Res.* **2019**, *189*, 46–53. [[CrossRef](#)]
43. Abbott, M.L.; Schmid, K.L.; Strang, N.C. Differences in the accommodation stimulus response curves of adult myopes and emmetropes. *Ophthalmic Physiol. Opt.* **1998**, *18*, 13–22. [[CrossRef](#)]
44. Swiatczak, B.; Schaeffel, F. Myopia: Why the retina stops inhibiting eye growth. *Sci. Rep.* **2022**, *12*, 21704. [[CrossRef](#)]
45. Rozema, J.; Dankert, S.; Iribarren, R. Emmetropization and non-myopic eye growth. *Surv. Ophthalmol.* **2023**, *68*, 759–783. [[CrossRef](#)]

**Disclaimer/Publisher’s Note:** The statements, opinions and data contained in all publications are solely those of the individual author(s) and contributor(s) and not of MDPI and/or the editor(s). MDPI and/or the editor(s) disclaim responsibility for any injury to people or property resulting from any ideas, methods, instructions or products referred to in the content.

Reproduced with permission of copyright owner. Further reproduction  
prohibited without permission.